Regular Article

blood

HEMATOPOIESIS AND STEM CELLS

An autonomous *CEBPA* enhancer specific for myeloid-lineage priming and neutrophilic differentiation

Roberto Avellino,[1] Marije Havermans,[1] Claudia Erpelinck,[1] Mathijs A. Sanders,[1] Remco Hoogenboezem,[1] Harmen J. G. van de Werken,[2-4] Elwin Rombouts,[1] Kirsten van Lom,[1] Paulina M. H. van Strien,[1] Claudia Gebhard,[5,6] Michael Rehli,[5,6] John Pimanda,[7] Dominik Beck,[7] Stefan Erkeland,[1,8] Thijs Kuiken,[9] Hans de Looper,[1] Stefan Gröschel,[1,10] Ivo Touw,[1] Eric Bindels,[1] and Ruud Delwel[1]

[1]Department of Hematology, [2]Cancer Computational Biology Center, [3]Department of Cell Biology, and [4]Department of Urology, Erasmus University Medical Center, Rotterdam, The Netherlands; [5]Department of Internal Medicine III and [6]Regensburg Centre for Interventional Immunology, University Hospital Regensburg, Regensburg, Germany; [7]Prince of Wales Clinical Schools and Lowy Cancer Research Centre, The University of New South Wales, Sydney, NSW, Australia; [8]Department of Immunology and [9]Department of Viroscience, Erasmus University Medical Center, Rotterdam, The Netherlands; and [10]Department of Translational Oncology, National Center for Tumor Diseases, Deutsches Krebsforschungszentrum (DKFZ), Heidelberg, Germany

Key Points

- The *CEBPA* locus harbors 14 enhancers of which distinct combinations are active in different *CEBPA*-expressing tissues.
- A +42-kb enhancer is required for myeloid-lineage priming to drive adequate *CEBPA* expression levels necessary for neutrophilic maturation.

Neutrophilic differentiation is dependent on *CCAAT* enhancer-binding protein α (C/EBPα), a transcription factor expressed in multiple organs including the bone marrow. Using functional genomic technologies in combination with clustered regularly-interspaced short palindromic repeat (CRISPR)/CRISPR-associated protein 9 genome editing and in vivo mouse modeling, we show that *CEBPA* is located in a 170-kb topological-associated domain that contains 14 potential enhancers. Of these, 1 enhancer located +42 kb from *CEBPA* is active and engages with the *CEBPA* promoter in myeloid cells only. Germ line deletion of the homologous enhancer in mice in vivo reduces *Cebpa* levels exclusively in hematopoietic stem cells (HSCs) and myeloid-primed progenitor cells leading to severe defects in the granulocytic lineage, without affecting any other *Cebpa*-expressing organ studied. The enhancer-deleted progenitor cells lose their myeloid transcription program and are blocked in differentiation. Deletion of the enhancer also causes loss of HSC maintenance. We conclude that a single +42-kb enhancer is essential for *CEBPA* expression in myeloid cells only. (*Blood.* 2016;127(24):2991-3003)

Introduction

All cell types in the bone marrow are derived from a pool of hematopoietic stem and progenitor cells (HSPCs) that sustain blood cell development throughout the life of an organism. Prior to lineage commitment and differentiation, HSPCs undergo chromatin changes brought about by lineage-specific transcription factors (LTFs) to prime and activate lineage-specific gene expression programs.[1] Priming of cell lineages involves the accessibility and activity of cell type-specific enhancers by LTFs to regulate the expression of genes responsible for any given cell lineage.[2-4]

Cell-lineage priming occurs during cell-fate decisions which are mainly dependent on the concentration or dosage of LTFs.[5-7] For instance, lymphoid-primed progenitors have high concentrations of lymphoid-related LTFs such as IKAROS, E47, and EBF that bind and activate lymphoid-specific enhancers to induce lymphoid development.[8] To skew differentiation toward myelopoiesis, these factors become negatively regulated upon increased dosage of the inhibitors of differentiation transcription factors (TFs), in order to favor increased PU.1 levels and promote myeloid commitment.[9] The leucine zipper TF CCAAT enhancer-binding protein α (C/EBPα) instructs myeloid differentiation via the priming and activation of myeloid-associated genes in HSPCs[10] and competes for genomic occupancy with other TFs, such as PU.1 and GATA2 in the myeloid-erythroid progenitor compartment, to favor neutrophilic differentiation over monocytic, erythroid, and megakaryocytic cell differentiation.[11,12] The important role of C/EBPα in myelopoiesis is substantiated by the diverse oncogenic mechanisms that target C/EBPα levels and function in various subsets of acute myeloid leukemia (AML).[13-18] Moreover, *Cebpa* knockout mouse models show severe myeloid defects in the bone marrow[19] as well as in several other organs including the liver,[20] lung,[21] bone tissue[22] as well as in epithelium of the gut,[23] implying its broad role as a differentiation TF in several organs. The broad role of C/EBPα as a differentiation mediator in multiple tissues suggests that *CEBPA* is under the control of tissue-specific transcriptional regulatory mechanisms.[24] Transcription regulation occurs in a hierarchical order of multistep processes that involve the structural organization of the genome to regulate gene expression programs via tissue-specific enhancers.[25-27]

Submitted January 28, 2016; accepted March 2, 2016. Prepublished online as *Blood* First Edition paper, March 10, 2016; DOI 10.1182/blood-2016-01-695759.

The online version of this article contains a data supplement.

There is an Inside *Blood* Commentary on this article in this issue.

The publication costs of this article were defrayed in part by page charge payment. Therefore, and solely to indicate this fact, this article is hereby marked "advertisement" in accordance with 18 USC section 1734.

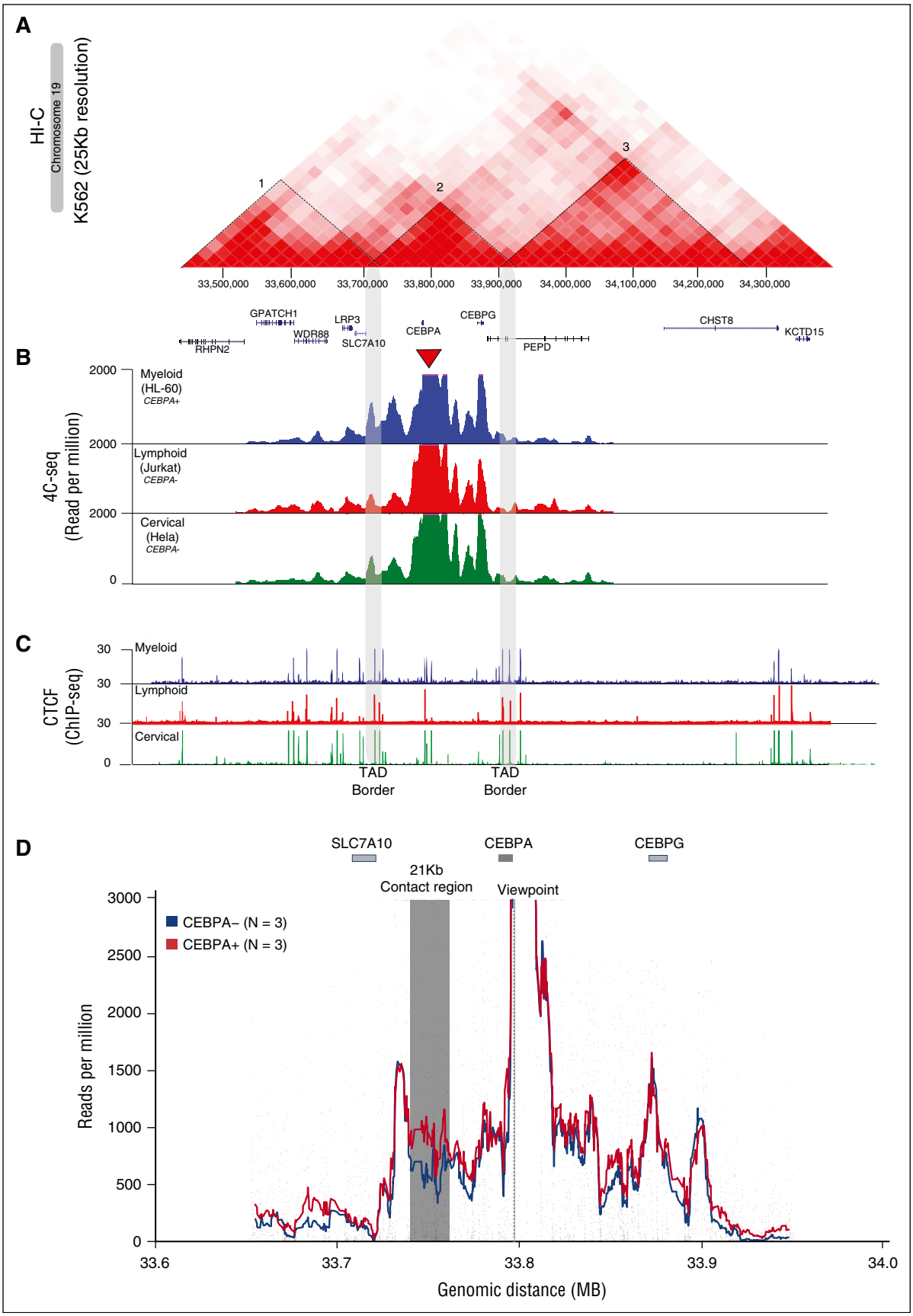

Figure 1. The *CEBPA* promoter contacts multiple intra-TAD genomic sites. Stronger interaction with a 21-kb genomic region in *CEBPA*-expressing myeloid cells. (A) HI-C heatmap matrix (25-kb resolution) in the K562 cell line on chromosome 19 reveals a 170-kb *CEBPA* TAD (2), which is flanked by TADs 1 and 3. The *CEBPA* TAD also contains *CEBPG* and part of *SLC7A10*. (B) Normalized 4C-seq profiles of myeloid *CEBPA*$^{+}$ HL-60 (blue), lymphoid *CEBPA*$^{-}$ Jurkat (red) and cervical *CEBPA*$^{-}$ HeLa (green)

In this study, we investigated how *CEBPA* transcription is regulated during myelopoiesis. We show that the *CEBPA* locus harbors, in total, 14 enhancers and we asked whether *CEBPA* contacts tissue-specific enhancers in different *CEBPA*-expressing cell types. Using a combination of functional genomics and clustered regularly-interspaced short palindromic repeat (CRISPR)/CRISPR-associated protein 9 (Cas9) genome editing in human cell lines and mouse models, we show that the +42-kb enhancer acts autonomously in myeloid-primed hematopoietic stem cells (HSCs) in the bone marrow to drive adequate *CEBPA* expression levels necessary for full neutrophilic maturation.

Materials and methods

Cell lines and cell culture

Cell lines were cultured as follows: U937, THP-1, Raji, Jurkat in 90% RPMI 1640 and 10% fetal calf serum (FCS); Hep3B, H292, and HepG2 80% RPMI 1640 and 20% FCS; HEK293T and HeLa in 90% Dulbecco modified Eagle medium and 10% FCS. All cell lines were supplemented with 50 U/mL penicillin and 50 μg/mL streptomycin.

High-resolution circularized chromatin conformation capture sequencing

High-resolution circularized chromatin conformation capture sequencing (4C-seq) was conducted as previously described.[28] In brief, 10×10^6 cells were crosslinked with 2% formaldehyde for 10 minutes at room temperature. Glycine (0.125 M) was added to quench the crosslinking reaction and cells were centrifuged and suspended in lysis buffer to disrupt membranes and isolate chromatin. A primary 4-base cutter, either DPNII or NLAIII, was used for digestion, followed by diluted ligations. After precipitation, chromatin was further subjected to a second round of digestions with a different 4-base cutter (either Csp6I or BFAII) and ligated to small-circularized plasmids. Primers for the *CEBPA* viewpoint (forward, TACTGCTTCTTTACTGC GATC; reverse, CAAGCAGAAGACGGCATACGA) and for the 21-kb contact domain viewpoint (forward, GCCCAGGAGCCTGTGAGATC; reverse, ACTCTGAGTGCAGAGAGGAG) were designed as previously reported.[28] Primers were designed for 4C-seq taking the viewpoints at the 5′ border of the 170-kb topological-associated domain (TAD) near *CEBPG* (forward, TTTTACAAGTCACAGGGATC; reverse, ACGTCCTCTGT ATTGCCTAG) and the 3′ border of the TAD, near the promoter of *SLC7A10* (forward, CCAGCACACACTGCAAGATC; reverse, GGAGGGAGTTCTGT GTGG). Inverse polymerase chain reaction (PCR) was carried out to amplify sample libraries that were pooled and spiked with 40% PhiX viral genome sequencing library to increase sample diversity. Multiplexed sequencing was performed on the HiSeq2500 platform. 4C-seq data analysis is explained in the supplemental Methods (available on the *Blood* Web site).

ChIP sequencing

Chromatin immunoprecipitation (ChIP) experiments were performed as previously described.[29] Cells were crosslinked at room temperature for 10 minutes with 1% formaldehyde and sonicated to shear the chromatin. Immunoprecipitation of crosslinked chromatin was performed overnight at 4°C with antibodies directed against the histone mark H3K27ac, the coactivator p300, and TFs including RUNX1, LMO2, PU.1, ERG, TAL1, and SCL, or an equal amount of isotype immunoglobulin G (IgG) as background control (http://149.171.101.136/python/BloodChIP/search.html). Descriptions detailing the preparation of library preparation, genome alignment, and peak calling are included in the supplemental Methods.

Flow cytometry and sorting

Flow cytometry and sorting were carried out on the LSRII and the FACSAria IIIU (Becton Dickinson), respectively, using the following fluorescent antibodies: CD11B- allophycocyanin (APC)/GR1–fluorescein isothiocyanate/B220-phycoerythrin (PE)/CD45 peridinin chlorophyll CY5/LIN bio cocktail streptavidin–Pacific Orange/cKIT-APC/SCA1-PB/CD48–fluorescein isothiocyanate/CD150-PE-CY7/CD16-32APC-CY7/CD34-PE. All antibodies were purchased from BD Biosciences and Biologend. Sorted fractions were collected in 500 μL of phosphate-buffered saline with 5% FCS, spun down, and resuspended in 800 μL of TRIzol and used for RNA sequencing (RNA-seq).

RNA-seq

Total sample RNA was extracted using TRIzol with Genelute LPA (Sigma) as a carrier, and the SMARTer Ultra Low RNA kit for Illumina Sequencing (Clontech) was used for complementary DNA synthesis according to the manufacturer's protocol. The complementary DNA was sheared with the Covaris device and further processed according to the TruSeq RNA Sample Preparation, v2 Guide (Illumina). The amplified sample libraries were subjected to paired-end sequencing (2×75 bp) and aligned against mm10 using TopHat, v2.[30,31] Alignment and processing of RNA-seq data are documented in the supplemental Methods.

Luciferase reporter assays

The full canonical *CEBPA* promoter was PCR amplified from genomic DNA (gDNA) and cloned into the pGL4.11 (Luc2CP) (*Eco*RV/*Hin*dIII) (Promega) luciferase construct. The +9-kb or +42-kb enhancers were PCR amplified and cloned into pGL4.11 (luc2CP) (*Sal*1/*Bam*H1) 3′ of the luciferase gene in the same construct where the full canonical *CEBPA* promoter was cloned (see supplemental Methods for primer sequences). HEK293T cells were transfected with Lipofectamine 2000 (Invitrogen), U937 electroporated with Lonza Kit (Kit-C), Jurkat, K562, THP-1, HepG2, and H292 cells with X-tremeGENE HP DNA Transfection Reagent (Roche). Cells were harvested after 48 hours, and luciferase activity was measured with the Dual-Luciferase Reporter Assay System (Promega) on a Victor X3 plate reader (Perkin Elmer). All assays were measured in duplicates and performed minimally 3 times.

CRISPR in human cell lines

CRISPR in human cell lines and in mouse fertilized eggs was carried out as explained in the supplemental Methods.

Results

CEBPA interacts with multiple intergenic regions, one of which is only prominent in *CEBPA*$^+$ myeloid cells

Promoter-enhancer interactions occur within TADs and gene promoters confined within such a domain might share the same set of enhancers for transcriptional regulation.[32-35] HI-C sequencing data,[36] a comprehensive technique to capture the conformation of genomes,[32] shows that *CEBPA* is located in a 170-kb conserved TAD (labeled 2 in Figure 1A and supplemental Figure 1A) on chromosome 19. This TAD also contains *CEBPG* and the promoter of *SLC7A10*, located 5′ and 3′ of *CEBPA*, respectively (Figure 1A). To determine the interacting

Figure 1 (continued) cell lines. The viewpoint (red triangle) located at the *CEBPA* promoter shows multiple interacting sites confined to the *CEBPA*-TAD (borders marked in gray). (C) CTCF ChIP-seq (ENCODE) in the myeloid HL-60, lymphoid Jurkat, and cervical HeLa cell lines shows enrichment at the *CEBPA* TAD borders (gray) which overlap with the HI-C contact-matrix borders separating the *CEBPA*-containing TAD2 from TAD1 and TAD3. (D) Semiquantitative analysis of 4C-seq data to distinguish interacting regions occurring at higher contact frequencies in *CEBPA*$^+$ myeloid cells (orange; n = 3) compared with *CEBPA*$^-$ cells (blue; n = 3). The *CEBPA* viewpoint is marked with a dotted line. A specific region indicated in gray of around 21 kb located 3′ of *CEBPA* and with >250 reads per million shows a statistically significant higher contact frequency (FDR < 0.05) in *CEBPA*$^+$ as compared with *CEBPA*$^-$ cell lines.

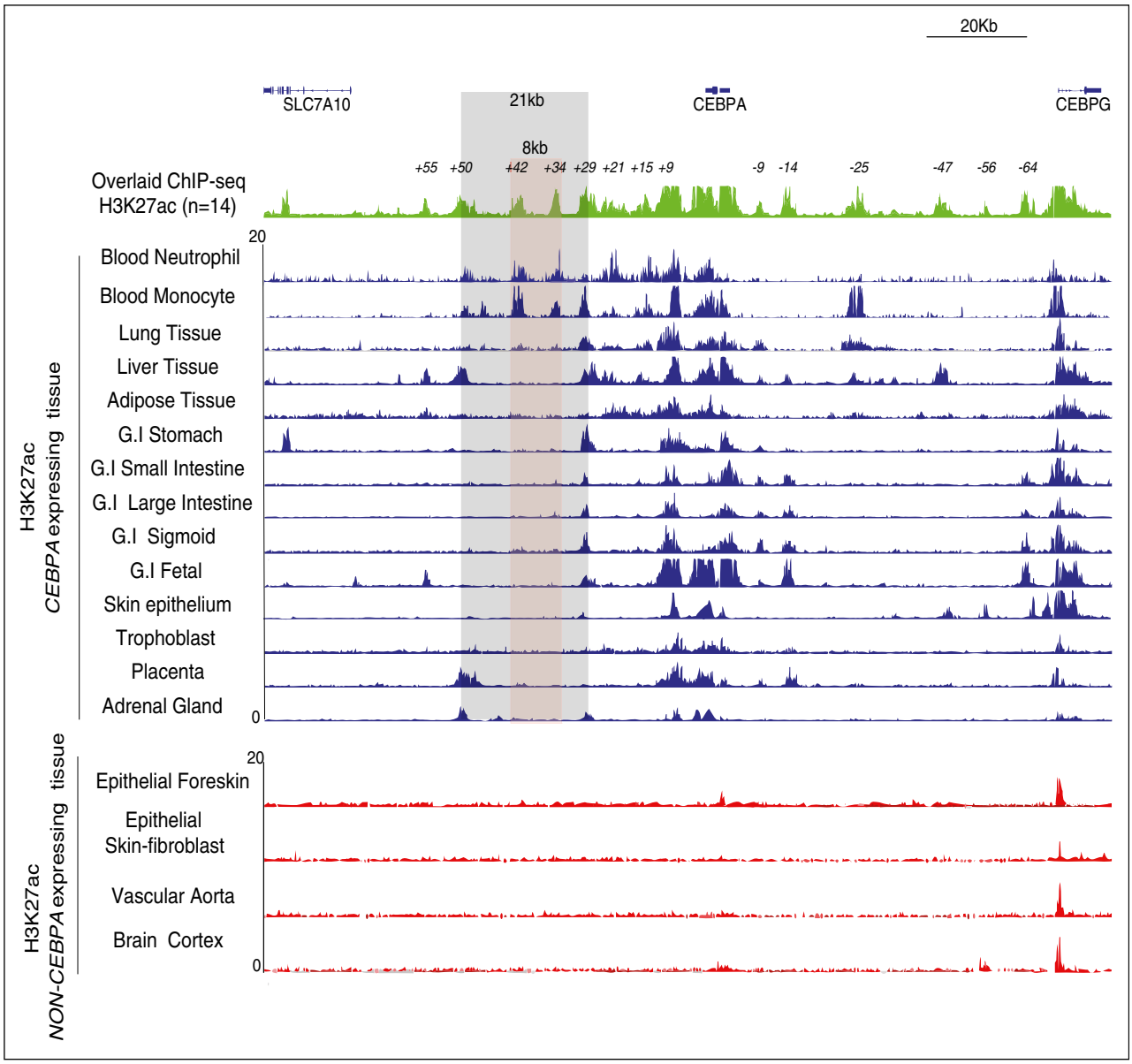

Figure 2. The *CEBPA* TAD exhibits a diverse combination of active enhancers in different *CEBPA*$^+$ tissues. ChIP-seq for H3K27ac conducted in terminally differentiated neutrophils and monocytes (in-house) was compared with publicly available ChIP-seq H3K27ac (www.roadmapepigenomics.org/). Superimposed H3K27ac (top; green) ChIP-seq profiles from 14 different *CEBPA*$^+$ tissue types shows 14 potential enhancers situated within the *CEBPA* TAD at 5′ (−9, −14, −25, −47, −56, −64 kb) and at 3′ (+9, +15, +21, +29, +34, +42, +50, +55 kb). Each individual *CEBPA*$^+$ tissue type (middle; blue) shows a different combinatorial set of active enhancers. *CEBPA*$^-$ tissue types (bottom; red) do not exhibit H3K27ac at the locus, except at *CEBPG*. An intergenic 8-kb hotspot (red) located within the 21-kb contact domain (gray), contains 2 potential enhancers (+34 kb and +42 kb) that are H3K27ac enriched in neutrophils and monocytes only. G.I, gastrointestinal.

regions within the 170-kb TAD (*CEBPA*-TAD) we applied high-resolution 4C-seq[28] taking the *CEBPA* promoter as a viewpoint (Figure 1B). Eight contact regions, located 5′ and 3′ of *CEBPA*, were found in all cell lines investigated,[37] that is, in *CEBPA*-expressing (*CEBPA*$^+$) myeloid cell lines HL-60, MOLM-1, U937, and THP-1, the lymphoid *CEBPA*$^-$ cell lines Jurkat and Raji, the lung *CEBPA*$^+$ cell line H292, and the cervical *CEBPA*$^-$ cell line HeLa (Figure 1B; supplemental Figure 1B). These contact domains varied in size between 10 and 22 kb (median = 11.65 kb) (supplemental Figure 1D). Taking the borders of the *CEBPA*-TAD as viewpoints (supplemental Figure 1C), 4C-seq revealed that the interactions were confined to this TAD. No significant interactions with the adjacent TADs 1 and 3 were found, in line with the binding of the architectural protein CTCF[36,38] to the borders of the *CEBPA*-TAD (labeled 1 and 3 in Figure 1A-C).

A region of 21-kb prominently contacts the *CEBPA* promoter

We next investigated whether any of the 8 contact regions identified by 4C-seq showed differential promoter interactions in *CEBPA*$^+$ myeloid cell lines compared with *CEBPA*$^-$ cells. A semiquantitative analysis of 4C-seq data was conducted by comparing 3 myeloid *CEBPA*$^+$ (MOLM-1, U937, and HL-60) with 3 nonmyeloid *CEBPA*$^-$ (Jurkat, Raji and HeLa) cell lines. The contact region of ~21 kb in size located 3′ of *CEBPA* (supplemental Figure 1D) showed a more significant interaction (false discovery rate [FDR] < 0.05) in the *CEBPA*$^+$ cell

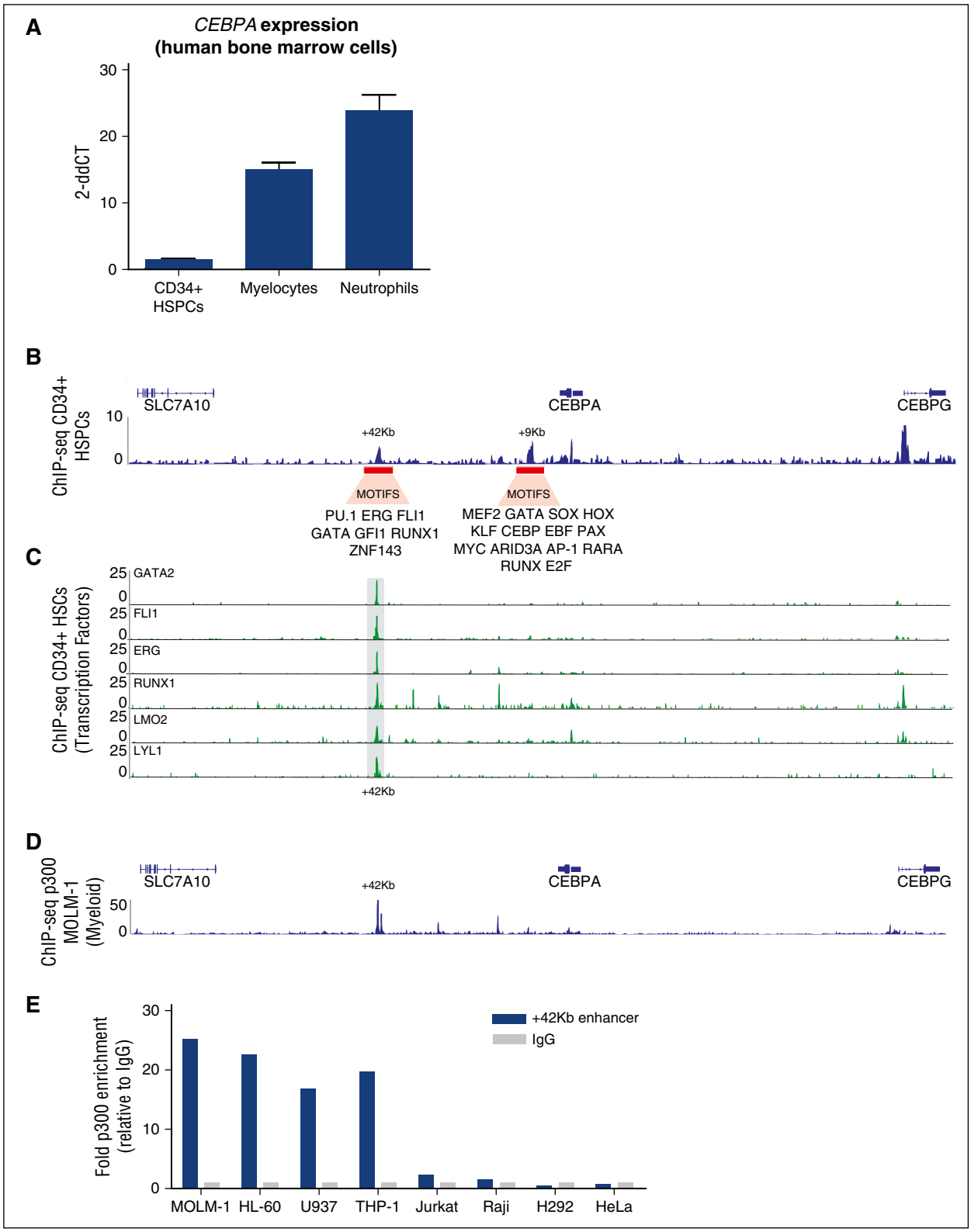

Figure 3. The +42-kb region is specifically H3K27ac marked in CD34$^+$ HSCs. (A) *CEBPA* mRNA expression determined by qPCR in FACS-sorted populations of normal CD34$^+$ bone marrow cells, metamyelocytes, and neutrophils (n = 3). (B) H3K27ac ChIP-seq in CD34$^+$ cells, obtained from GCSF-mobilized peripheral blood cells, reveals enrichment at the +9-kb and +42-kb enhancers. Motifs that correspond to specific TF-binding sites are depicted underneath each enhancer (for details, see supplemental Figure 3A). (C) ChIP-seq for the indicated transcription factors carried out in CD34$^+$ cells shows specific binding at the +42-kb enhancer. (D) ChIP-seq for p300 in MOLM-1 *CEBPA*$^+$ cell line MOLM-1 reveals the strongest interaction at +42 kb. (E) ChIP-qPCR shows p300 enrichment within the +42-kb region in the *CEBPA*-expressing cell lines MOLM-1, U937, HL-60, THP-1, but not in the *CEBPA*$^-$ hematopoietic cell lines Jurkat and Raji, CEBPA$^+$ lung cell line H292, and CEBPA$^-$ cervical cell line HeLa. Enrichment was calculated as fold change relative to IgG control.

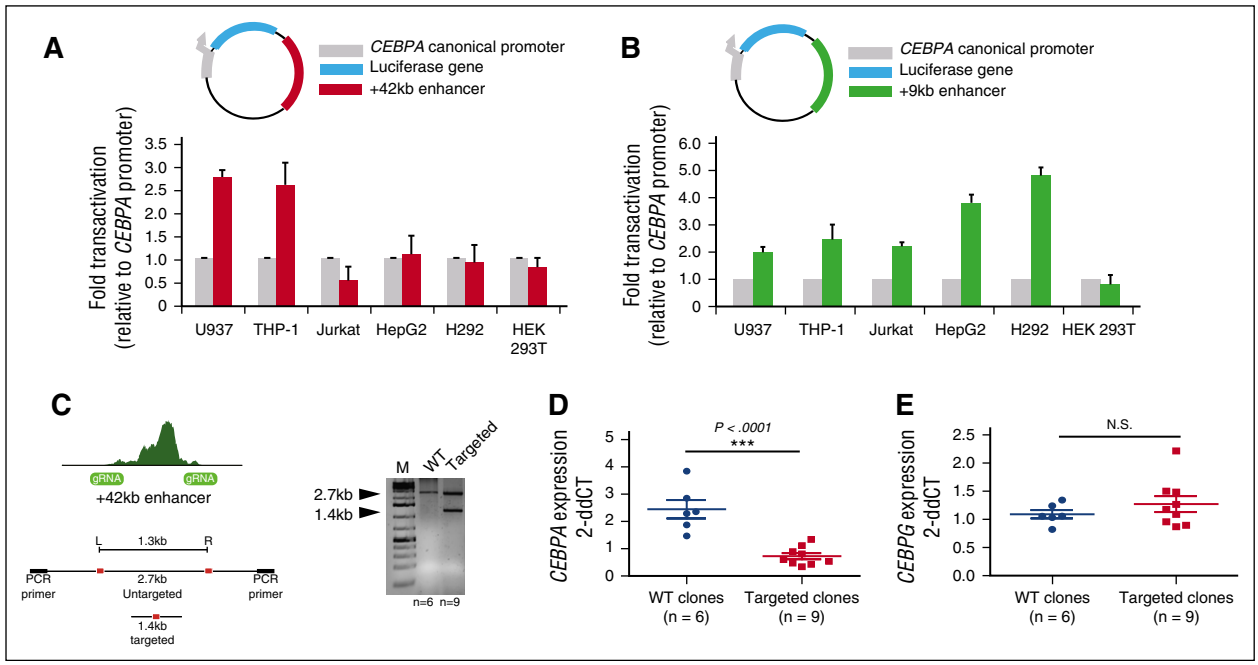

Figure 4. The +42-kb enhancer is a myeloid-specific *CEBPA* transcriptional activator. (A-B) The +42-kb and +9-kb enhancer were cloned 3′ of a luciferase reporter gene under the control of the full canonical *CEBPA* promoter. Results are presented as fold change of the +42-kb enhancer in combination with the *CEBPA* promoter (blue = myeloid; red = lymphoid; green = $CEBPA^+$ nonhematopoietic; orange = $CEBPA^-$ nonhematopoietic cell lines) relative to *CEBPA* promoter alone (gray). (C) gRNA for the CRISPR/Cas9 system were designed to flank the p300 and TF-binding sites within the +42-kb enhancer. Single-cell clones were generated and genotyped using a PCR strategy. (D-E) WT clones (n = 6) and homozygous clones (n = 9) were selected and qPCR for *CEBPA* mRNA expression and for *CEBPG* was conducted. Statistical significance to compare mRNA expression levels between WT and homozygous clones for both genes under investigation, was carried out using the 2-tailed Student's *t* test. ***$P < .0001$; N.S., not significant.

lines compared with $CEBPA^-$ cells (Figure 1D). In contrast, no major interaction differences were observed for the other *CEBPA* promoter-interacting regions. A reciprocal 4C-seq experiment using the 21-kb contact region as a viewpoint confirmed that the interaction with the *CEBPA* gene occurred at a higher frequency in $CEBPA^+$ myeloid cell lines (FDR < 0.05) (supplemental Figure 1E). These findings show that a distant region of 21 kb interacts with *CEBPA* prominently in $CEBPA^+$ myeloid cells, suggesting a myeloid-specific chromatin conformation at this region.

Two potential enhancers with myeloid preference located within the 21-kb contact region

To identify regions of active chromatin in peripheral blood neutrophils and monocytes, we conducted H3K27ac ChIP-seq and compared the determined H3K27ac profiles to those obtained from public available data derived from other human primary $CEBPA^+$ (n = 12) and $CEBPA^-$ (n = 4) tissues (http://www.roadmapepigenomics.org/). The H3K27ac ChIP-seq profiles revealed 14 potential enhancers within the *CEBPA*-TAD, located upstream and downstream of *CEBPA* (Figure 2 green profile). Each tissue investigated harbored a distinct combination of H3K27ac marked regions, suggesting tissue specificity and differential regulation of *CEBPA* expression (Figure 2 blue profiles). Tissues which do not express *CEBPA* were all devoid of H3K27ac marked sites within the *CEBPA*-TAD (Figure 2 red profiles), except for the *CEBPG* promoter.[39,40] Of these 14 potential enhancers, 10 located 5′ (−9 kb, −4 kb, −25 kb, −47 kb, and −64kb) and 3′ (+9 kb, +29 kb, +34 kb, +42 kb, +50 kb) of *CEBPA* are found within the 8 contact regions identified by 4C-seq (supplemental Figure 2). The +34-kb and the +42-kb regions were exclusively H3K27ac marked in neutrophils and monocytes. These 2 regions are located within the 21-kb large contact region that showed increased interaction in myeloid cells (Figure 1D). The +9-kb region is H3K27ac marked in all the *CEBPA*-expressing tissues investigated, suggesting a tissue-broad role in *CEBPA* regulation (Figure 2). These findings show that from a total of 14 potential enhancers located within the *CEBPA*-TAD, the +34-kb and +42-kb regions appear to be myeloid specific, suggesting the presence of an enhancer-rich chromatin site important for *CEBPA* transcriptional regulation.

The +42-kb enhancer is occupied by hematopoietic-specific transcription factors in HSPCs

CEBPA is expressed at low levels in $CD34^+$ progenitor cells and increases upon neutrophilic maturation (Figure 3A). The low *CEBPA* expression levels in $CD34^+$ progenitor cells (Figure 3A) correlate with the number of potential enhancers found by H3K27ac ChIP-seq (ENCODE),[41] that is, only the +42-kb and the +9-kb potential enhancers are active at this stage of hematopoiesis (Figure 3B). Motif analysis revealed that the +42-kb enhancer contains DNA-binding motifs (a CTCF-interacting zinc finger transcription factor[42]) and multiple HSPC-related (TFs) (supplemental Figure 3A). In contrast, the +9-kb enhancer contains DNA-binding motifs corresponding to a universal set of TFs (supplemental Figure 3A). Furthermore, the HSPC-related LTFs and other TFs including LYL11, RUNX1, GATA2, FLI1, ERG, and LMO2[6,43] bind the +42-kb region in $CD34^+$ cells (Figure 3C). Recruitment of p300 to enhancers is highly suggestive of enhancer activity.[44] ChIP-seq in the $CEBPA^+$ MOLM-1 cell line demonstrated strong binding of the histone acetyltransferase p300 to the +42-kb enhancer (Figure 3D). This binding was also demonstrated by ChIP–quantitative PCR (qPCR) in the $CEBPA^+$ myeloid cells HL-60, U937, and THP-1 (Figure 3E). No binding was found in the lymphoid cell lines Jurkat and Raji or the $CEBPA^+$

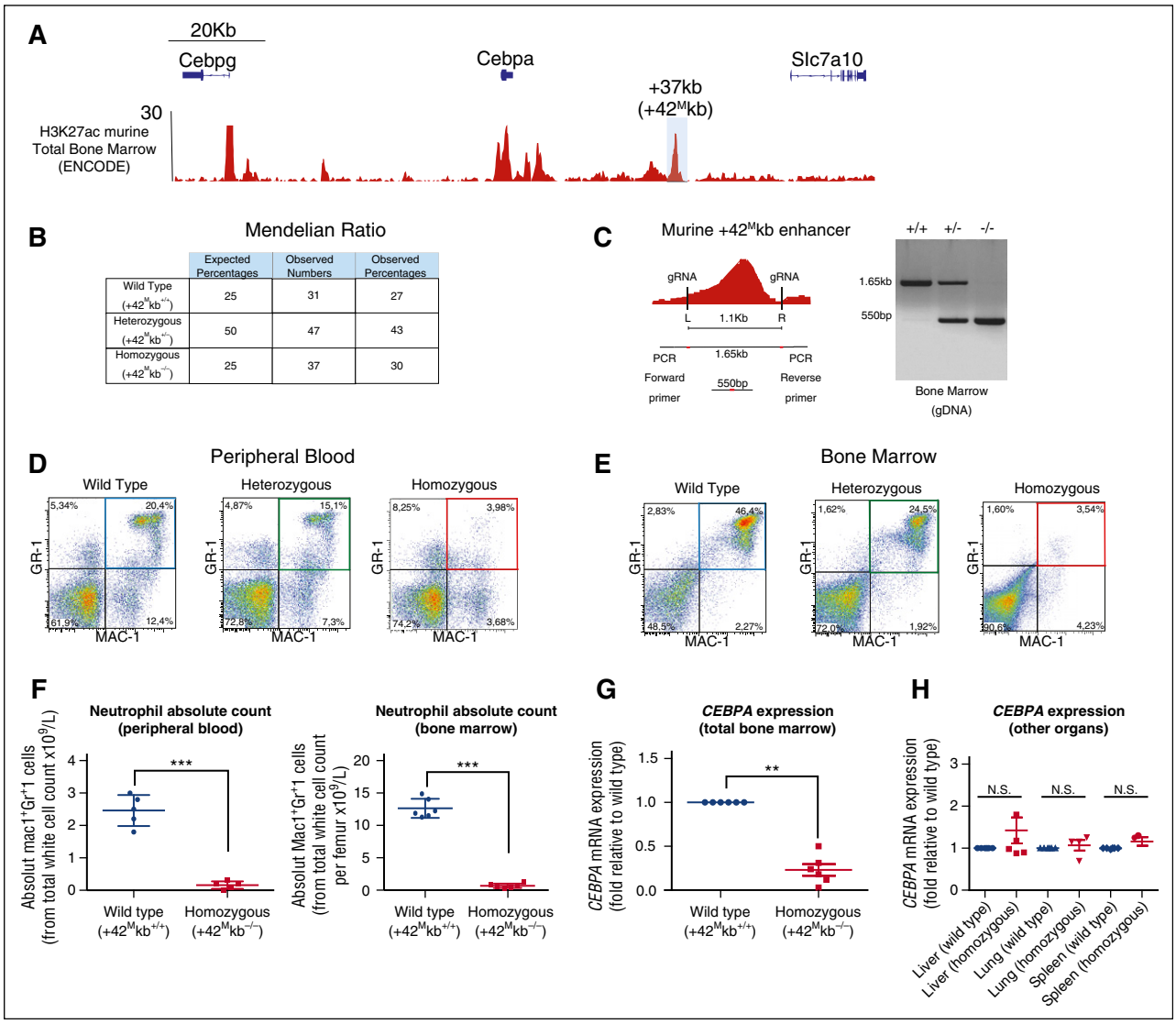

Figure 5. +37-kb deleted mice (+42Mkb) show low *Cebpa* levels and develop neutropenia. (A) ChIP-seq H3K27ac in murine total bone marrow (ENCODE) shows multiple regions of open chromatin. A region located at +37 kb in mice is highly homologous (supplemental Figure 5A) to the human +42-kb enhancer and is H3K27ac marked. (B) Table showing Mendelian ratios. (C) PCR genotyping using primers flanking the gRNAs generate an amplicon of 1.65 kb on the intact/WT allele and an amplicon of 550 bp on the deleted/rearranged allele. (D-E) Flow cytometric analysis to distinguish neutrophils in peripheral blood or bone marrow of WT (blue), heterozygous (green), and homozygous (red) mice using the myeloid differentiation markers Mac1 and GR1. (F) Neutrophil absolute counts in peripheral blood and bone marrows of WT and homozygous mice. (G) *Cebpa* mRNA expression from total bone marrow obtained from WT (n = 6) or homozygous +42Mkb knockout mice (n = 6) is presented as fold change. (H) *Cebpa* mRNA expression from liver, lung, and spleen does not show significant changes. ***$P < .0001$; **$P < .001$; N.S., not significant.

nonhematopoietic cell lines H292 (lung) and HeLa (cervical). Together, our data show that the +42-kb enhancer is a critical region highly occupied by a HSPC-related TF complex that potentially initiates *CEBPA* expression in $CD34^+$ progenitor cells.

The +42-kb enhancer regulates *CEBPA* in myeloid cells

We next determined the activity of the +42-kb enhancer using luciferase reporter assays. The +42-kb enhancer was cloned into a luciferase reporter construct driven by the *CEBPA* promoter and its activity was investigated in different cell lines (Figure 4A). A 2.5-fold increase of luciferase activity was observed in the myeloid cell lines U937 and THP-1, compared with the luciferase-reporter driven by the *CEBPA* promoter only. The +42-kb enhancer was not active in nonmyeloid cell lines Jurkat, HepG2, H292, or HEK293T (Figure 4A). In contrast, the activity of the +9-kb enhancer was more general across different cell types (Figure 4B). Using CRISPR/Cas9 genome-editing technology, we next generated guide RNAs (gRNAs) flanking the TF and the p300-binding region of the +42-kb enhancer (~800 bp) and coelectroporated them with Cas9 into the myeloid cell line THP-1. Targeted THP-1 cells generated heterozygous clones (Figure 4B), which were further tested for *CEBPA* expression by qPCR. Deletion of the +42-kb enhancer resulted in twofold to fourfold reduced *CEBPA* transcript levels as compared with wild-type (WT) controls (Figure 4C). No changes in *CEBPG* messenger RNA (mRNA) expression levels were observed (Figure 4D). *SLC7A10*, located 5′ of the 170-kb *CEBPA* TAD, is not expressed in THP-1 cells (data not shown). In contrast to the effects observed in THP-1 cells, deletion of the +42-kb enhancer in the Hep3B hepatocyte cell line revealed no changes in *CEBPA* or *CEBPG* expression compared with WT clones (supplemental Figure 4). These results suggest a tissue-specific role of the +42-kb enhancer in the regulation of *CEBPA* levels in myeloid cells.

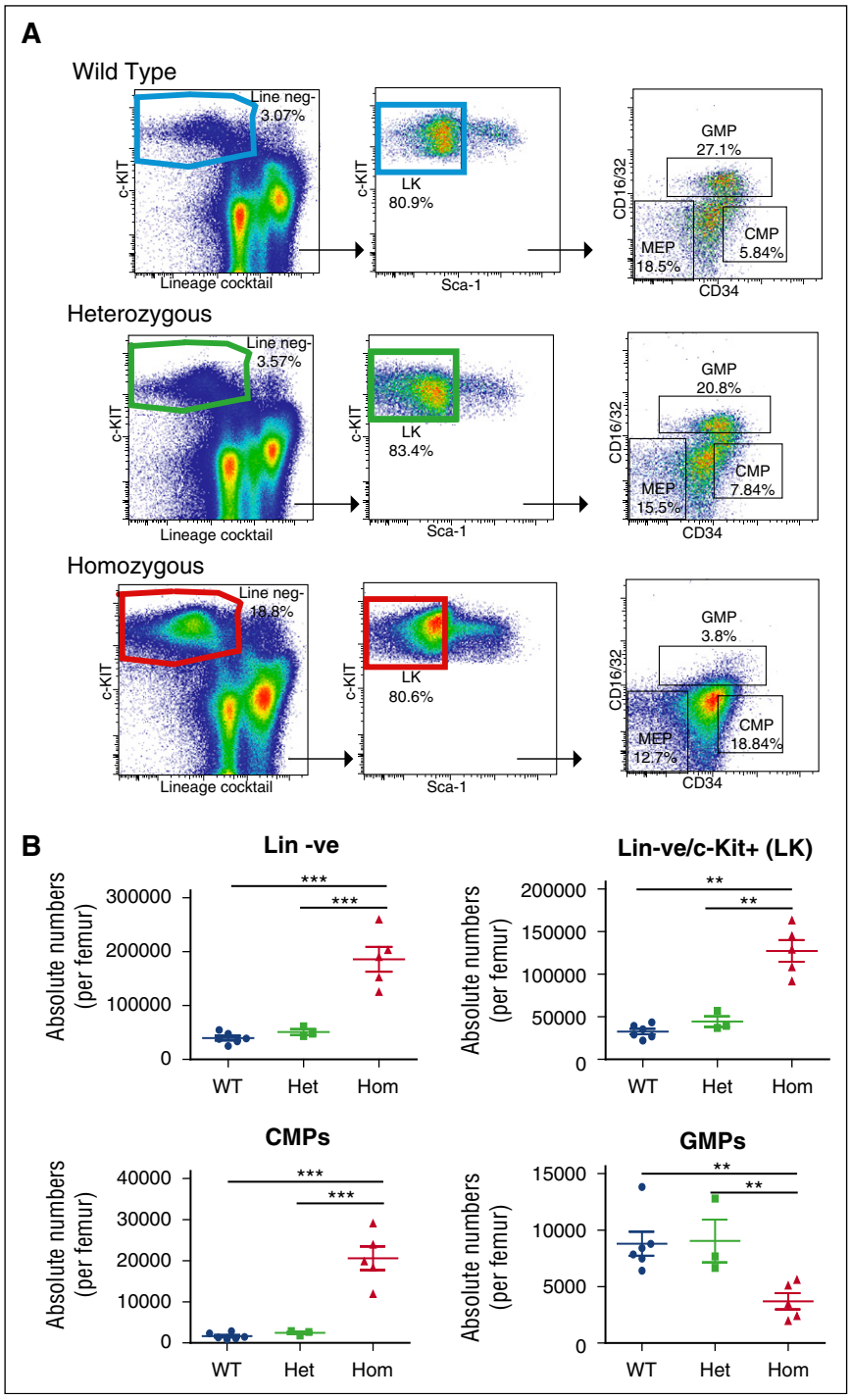

Figure 6. Reduction in GMPs, increase in CMPs, and loss of GCSF response in +42^{M}kb enhancer deleted bone marrow. (A) Lineage-negative cKIT^{+}Sca-1^{-} (LK) cells were derived from gated c-KIT^{+} cells. The myeloid progenitor cell population including CMP, GMP, and MEP was characterized using CD34 and CD16/32 markers gated from LK cells. (B) Absolute numbers for lineage-negative cells, LK, CMP, and GMP cell populations were calculated from bone marrow white cell count per femur. (C) *Cebpa* expression measured by RNA-seq expressed as FPKM values derived for WT and homozygous mice in CMP (2wt vs 3hom) and GMP (2wt vs 2hom) sorted fractions. (D) Csf3r expression in total bone marrow by qPCRs, presented as fold change between WT (n = 3) and homozygous (n = 3) mice. RNA-seq analysis of *Csf3r* in FACS-sorted CMP and GMP cell populations with values expressed as FPKM. (E) Numbers of CSF3-stimulated colonies per 10 000 cells plated obtained from WT bone marrow or from +42^{M}kb homozygous deleted mice. Colony numbers represent the average of 3 independent experiments. Representative microphotographs of colonies show differences in sizes and numbers between WT and homozygous mice. FPKM, fragments per kilobase of transcript per million mapped reads.

In vivo deletion of the murine +42-kb homologous enhancer causes neutropenia

We hypothesized that deletion of the +42-kb enhancer in vivo would cause neutropenia due to a selective decrease of *Cebpa* levels in myeloid progenitors, leaving other *Cebpa* expressing organs unaffected. A region located +37 kb from the mouse *Cebpa* transcriptional start site shows ~90% homology with the human +42-kb region and is H3K27ac enriched in mouse bone marrow (Figure 5A; supplemental Figure 5A; ENCODE).[41] Applying CRISPR/Cas9 nickase technology, we generated 3 +37 kb (here designated +42^{M}kb) knockout mouse lines (supplemental Figure 5B). Genotyping confirmed germ line deletion of the enhancer in the 3 lines and revealed Mendelian distributions of WT (+42^{M}kb$^{+/+}$), heterozygous-deleted (+42^{M}kb$^{+/-}$), and homozygous-deleted (+42^{M}kb$^{-/-}$) mice (Figure 5B-C). In contrast to full *Cebpa* knockout mice,[19] homozygous +42^{M}kb$^{-/-}$ mice were viable after birth and histopathological analysis of 4- to 5-week-old mice did not reveal any major defects in lung, liver, or spleen tissue (data not shown). Flow cytometric analysis of blood and bone marrow showed a strong reduction of Mac1^{+}Gr1^{+} mature neutrophils in +42^{M}kb$^{-/-}$ mice compared with age-matched +42^{M}kb$^{+/-}$ and +42^{M}kb$^{+/+}$ control animals (Figure 5D-F). May-Grünwald staining of bone marrow cells

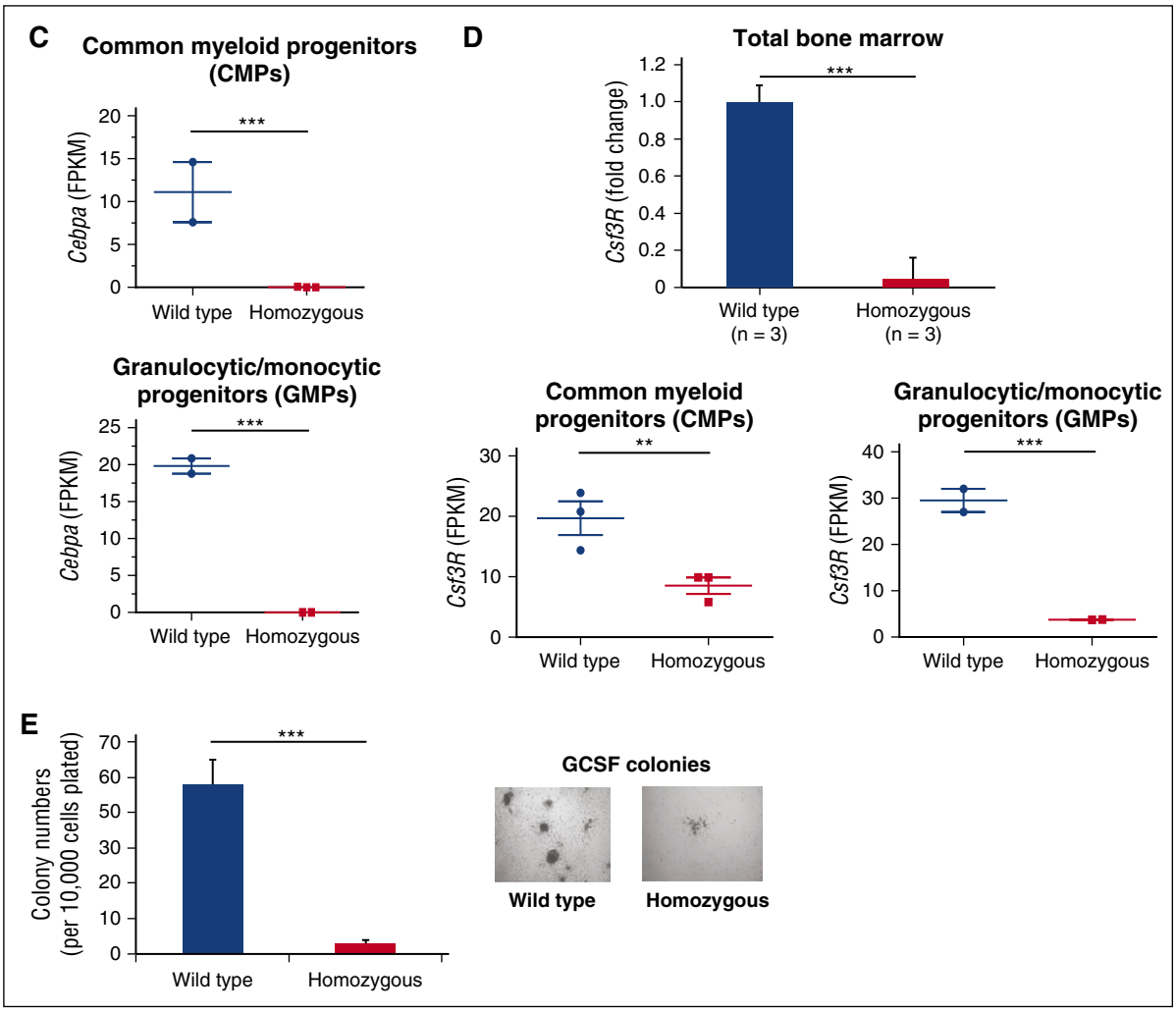

Figure 6. (Continued).

showed the reduction of neutrophils in $+42^{M}kb^{-/-}$ mice compared with control mice (supplemental Figure 5D). It is important to note that, in line with the fact that the neutrophil count was severely reduced, ~30% of the $+42^{M}kb^{-/-}$ mice died of bacterial infections 3 to 4 weeks after birth, as illustrated by the presence of bacteria in blood vessels of multiple tissues by histopathological analysis (supplemental Figure 5F). Other blood indices, including total white blood cell count and hemoglobin concentration revealed no differences between WT and mutant mice (supplemental Figure 5C-D). A slight increase in lymphocyte and monocyte counts was noticed, probably due to reduced space that is normally occupied by neutrophils in the bone marrow (data not shown). *Cebpa* transcript levels were 60% to 80% reduced in total bone marrow of $+42^{M}kb^{-/-}$ mice compared with WT control mice (Figure 5F), but no changes in expression were observed in *Cebpg* expression levels, although *Cebpa* knockout shows increase in *Cebpg* levels.[45] No decrease of *Cebpa* transcript levels was observed in lung, liver, and spleen of $+42^{M}kb^{-/-}$ mice (Figure 5G).

The $+42^{M}kb$ enhancer controls *Cebpa* expression in GMPs and CMPs

We investigated whether the reduced neutrophil numbers are preceded by a decrease in *Cebpa* levels in bone marrow progenitor cells. Flow cytometric analysis showed a significant reduction in absolute numbers of granulocytic/monocytic progenitors (GMPs) and a significant increase in common myeloid progenitor (CMP) numbers in the bone marrow of $+42^{M}kb^{-/-}$ mice compared with $+42^{M}kb^{+/+}$ controls (Figure 6A-B). We performed RNA-seq on sorted progenitor fractions and observed that *Cebpa* levels were reduced >100-fold in CMPs and GMPs in $+42^{M}kb^{-/-}$ (n = 3) compared with $+42^{M}kb^{+/+}$ (n = 3) mice (Figure 6C). *Cebpa* levels were low to absent in megakaryocytic/erythroid progenitor–sorted populations from $+42^{M}kb^{+/+}$ and $+42^{M}kb^{-/-}$ mice (data not shown). CMPs and GMPs derived from $+42^{M}kb^{+/+}$ and $+42^{M}kb^{-/-}$ mice also showed major differences in expression levels of myeloid-associated genes (Figure 6C; supplemental Figure 6A-B). One of these target genes is *Csf3r*, encoding the colony-stimulating factor receptor Csf3r, required for GMP survival and neutrophilic differentiation. *Csf3r* transcript levels were decreased 20-fold in total marrow, as well as in CMP and GMP fluorescence-activated cell sorter (FACS)-sorted fractions from $+42^{M}kb^{-/-}$ mice (Figure 6D). Consequently, bone marrow cells from $+42^{M}kb^{-/-}$ mice failed to form colonies in response to granulocyte colony-stimulating factor (GCSF) (Figure 6E). These data show that the enhancer is required at early stages of myeloid development and acts as a main activator of the CSF3-driven myeloid differentiation program.

Loss of HSCs and expansion of multipotent progenitors in +42^{M}kb$^{-/-}$ mice

We next investigated the effects of +42^{M}kb enhancer deletion on the distribution of HSCs and multipotent progenitor cells (MPPs) (Figure 7B). Absolute numbers of the lin^{-}Sca-1^{+}c-KIT^{+} (LSK) cells were significantly higher in +42^{M}kb$^{-/-}$ mice than in control mice (Figure 7A-B). RNA-seq of the LSK fractions revealed that *Cebpa* levels were several folds lower in +42^{M}kb$^{-/-}$ (n = 3) than in +42^{M}kb$^{+/+}$ LSK cells (n = 3) (Figure 7C). Within the LSK population, MPPs can be discriminated from short-term HSCs (ST-HSCs) and long-term HSCs (LT-HSCs) using signaling lymphocyte-activating molecule (SLAM) code CD48/CD150 markers. The lin^{-}CD48^{-}CD150^{+} LT-HSCs and lin^{-}CD48^{-}CD150^{-} ST-HSCs were reduced by 10-fold to 20-fold in +42^{M}kb$^{-/-}$ mice (Figure 7A-B). These changes are in line with data from Porse and colleagues using the Mx-cre *Cebpa* conditional knockout model, indicating that decreased CEBP/α levels disturbs the integrity of the HSC pool.[10] Conversely, a significant increase of the lin^{-}CD48^{+}CD150^{-} and lin^{-}CD48^{+}CD150^{+} MPP population was observed in +42^{M}kb$^{-/-}$ mice. These data show that the enhancer activity at the HSPC stage is essential to maintain constant *Cebpa* levels in myeloid-primed progenitors during the course of myelopoiesis.

Sustained proliferation of +42^{M}kb$^{-/-}$ bone marrow progenitor cells

To investigate the effects of +42^{M}kb enhancer deletion on the proliferative behavior of bone marrow progenitors, colony cultures were carried out using a combination of interleukin-3 (IL-3), IL-6, stem cell factor (SCF), and granulocyte-macrophage colony-stimulating factor (GM-CSF). No differences in primary colony numbers were observed between +42^{M}kb$^{-/-}$, +42^{M}kb$^{+/-}$, or +42^{M}kb$^{+/+}$ mice. +42^{M}kb$^{-/-}$ bone marrow cells could be serially replated, whereas +42^{M}kb$^{+/-}$ and +42^{M}Kb$^{+/+}$ cells underwent exhaustion (Figure 7D). Flow cytometric analysis revealed that the majority of the replated cells from +42^{M}kb$^{-/-}$ mice expressed lin^{-}CD48^{+} CD150^{-} MPP and lin^{-}CD16/32^{+}CD34^{+} GMP markers with minimal neutrophilic differentiation (Figure 7D).

Discussion

Applying functional genomics and genome editing in human hematopoietic cell lines, human bone marrow progenitors in vitro and mouse models in vivo, we show that a single, tissue-specific enhancer (1) is autonomously responsible for *CEBPA* expression in myeloid-primed HSCs, (2) initiates the myeloid gene expression program, and (3) is indispensable for neutrophil development.

Deletion of the +42^{M}kb enhancer in our model causes loss of *Cebpa* expression in the myeloid lineage and causes failure of the induction of complete neutrophilic differentiation. This suggests that the +42-kb enhancer initiates the myeloid program by acting as a highly occupied target region for HSC-related TFs (Figure 3) and thereby activates *Cebpa*.[46] Upon myeloid commitment, the intergenic site between *CEBPA* and *SLC7A10* contains multiple enhancers which become active during myeloid differentiation (Figure 2; supplemental Figure 5D), raising the question of whether these enhancers possess functional redundancy, thus, acting as shadow enhancers.[47,48] We postulate that (1) the +42-kb enhancer works autonomously at the HSPC stage to induce necessary *Cebpa* levels, (2) followed by activation of the myeloid transcription program inducing myeloid commitment, (3) upon myeloid commitment the other enhancers become active in order to serve as a transcription activation platform[49] and elevate *Cebpa* levels to a necessary level for terminal neutrophilic differentiation (supplemental Figure 8). We predict that upon deletion of the +42-kb enhancer the other enhancers within the locus will not become active (absence of H3K27ac) resulting in a block of differentiation.

The +42-kb enhancer deletion causes a complete lack of LT-HSCs and ST-HSCs. Therefore, the +42^{M}kb$^{-/-}$ mice behave like the previously reported Mx-Cre/*Cebpa* conditional knockout mice.[50] In these mice, as well as in other studies,[10,51] it has been demonstrated that *Cebpa* levels are critical to maintain HSC numbers and survival under a quiescent state. Given that only a small population of HSCs expresses *Cebpa*,[52] it remains unclear what causes the severe loss of HSCs upon deletion of either *Cebpa* or the +42^{M}kb enhancer. The LSK fraction (including the MPPs, LT-HSCs, and ST-HSCs) shows significant reduction of *Cebpa* levels in the +42^{M}kb$^{-/-}$ mice, suggesting a critical role for the enhancer in *Cebpa* regulation in LSKs. However, given that the MPP fraction (CD48^{+}CD150^{-}) constitutes the majority of the LSK population, *Cebpa* downregulation in the LSK fraction (Figure 7B) mainly reflects *Cebpa* level changes in the MPP population. Given that C/EBPα negatively regulates cell cycle genes to keep a constant balance of proliferation and differentiation,[53] it is possible that the block in differentiation leads to a constant demand for progenitor production, causing HSC exhaustion. Expression levels in LT-HSCs and ST-HSCs of *Cebpa* in the +42^{M}kb$^{-/-}$ mice are suggestive to confirm this hypothesis. In our model, the expansion of the progenitor population argues in favor of an increased progenitor state as a negative feedback mechanism to compensate for the differentiation block.

CEBPA is located in an enhancer-rich TAD and its promoter contacts 8 intergenic sites. One question to be addressed is which potential architectural proteins or protein complexes are involved in the +42-kb enhancer (or any of the other interacting enhancers) to *CEBPA* promoter interaction. The TAD is confined to a genomic region of 170 kb with borders demarcated by CTCF (Figure 1C), an architectural protein involved in looping interactions within and across TADs.[38,54,55] CTCF also binds to the promoter of *CEBPA*, possibly, by forming multiple extrusions of the 5′ and 3′ interacting intergenic sites of *CEBPA*.[56] The intergenic sites contacting *CEBPA* are highly enriched for H3K27ac thereby marking potential enhancers, but they lack CTCF or cohesion binding. From our motif analysis data (supplemental Figure 3), we found that the +42-kb enhancer harbors a ZNF143 DNA-binding motif (CAGCCTTCATG CATTG). ZNF143 is a zinc finger TF that associates with CTCF to allocate enhancers close to promoters and facilitate transcription regulation.[42] It is therefore possible that ZNF143 has implications in initiating this interaction by binding the +42-kb enhancer to associate with CTCF on the *CEBPA* promoter, thus causing the +42-kb enhancer-*CEBPA* promoter interaction (supplemental Figure 7). To test this hypothesis, functional experiments including genome editing of the ZNF143 binding site followed by 4C-seq are required to reveal the association between ZNF143 binding and *CEBPA* regulation in terms of a ZNF143-dependent *CEBPA* promoter to enhancer interaction.

Diverse oncogenic mechanisms that affect C/EBPα expression or function were reported in various subsets of AML.[13-18] Consequently, it is possible that mutations in the +42-kb enhancer could be related to transforming events. Therefore, a mutational screen of the regulatory elements of *CEBPA* is justified. The expansion of the MPP population in the enhancer-deleted mice suggests a preleukemic potential, which can only be confirmed by conducting serial transplantation

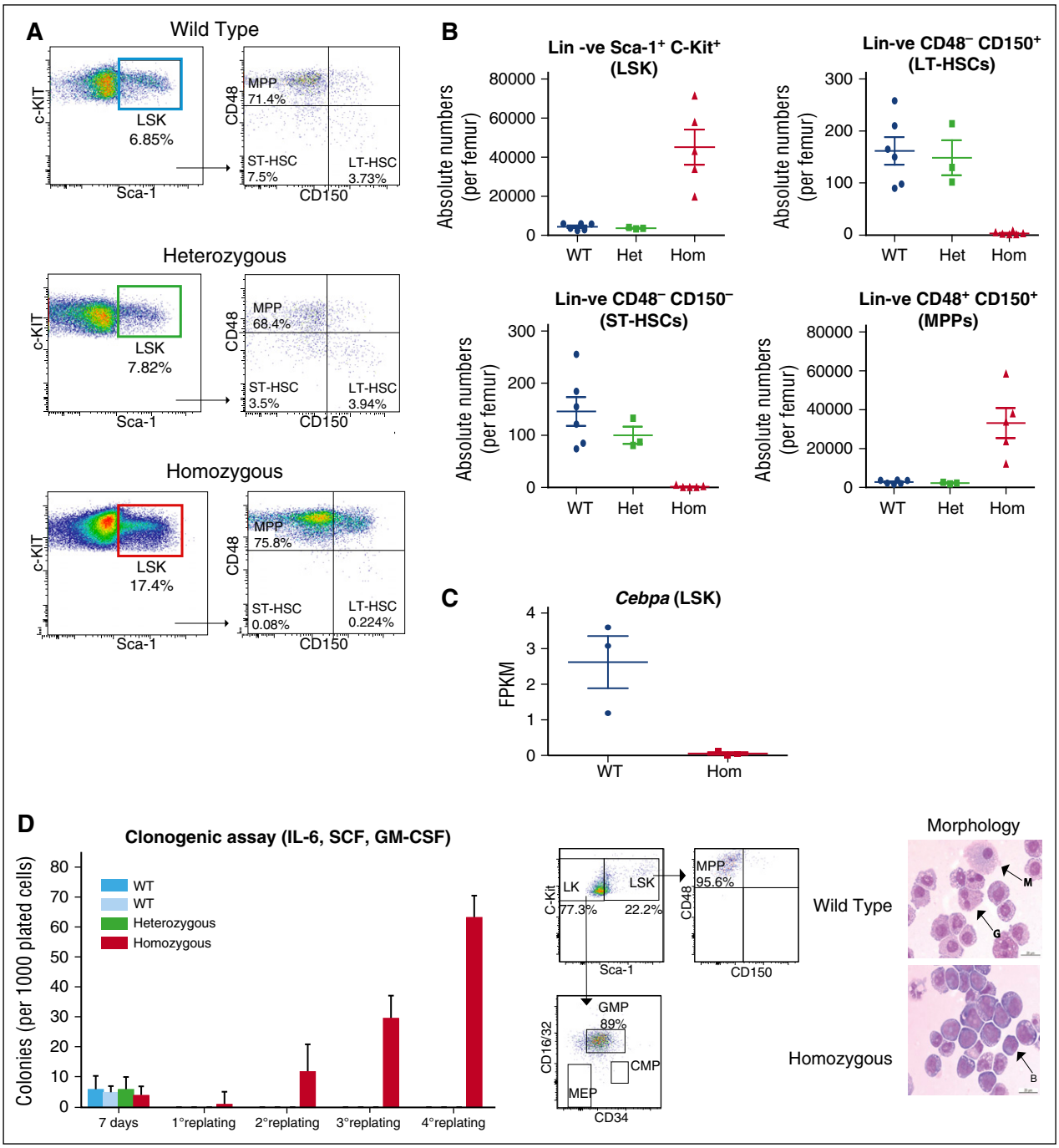

Figure 7. Loss of HSCs and expansion of multipotent progenitors in +42^{M} kb$^{-/-}$ mice. (A) SLAM CD48^{+}CD150^{+} markers were used to characterize cell distribution within the MPP, LT-HSC, and ST-HSC cell populations gated from lin^{-}Sca-1^{+}c-kit^{+} (LSK) cell populations. (B) Absolute cell numbers for LSK, MPP, LT-HSCs, and ST-HSCs were calculated from bone marrow white cell count per femur. (C) *Cebpa* expression by RNA-seq (FPKM values of WT vs homozygous mice). (D) Total bone marrow cells from WT, heterozygous, and homozygous mice were cultured in semisolid medium supplemented with IL-3, IL-6, SCF, and GM-CSF. Colonies were counted and replated every 7 days. FACS plots showing that the majority of cells grown under these conditions are mainly LK/GMP cells and, to a lesser extent, MPP/LSK cells. Morphological examination with May-Grünwald-Giemsa after 7 days distinguishes normal granulocytic and macrophage differentiation in WT cells as compared with homozygous cells that show blasts as the major cell population.

experiments. The sustained replating of the +42^{M}kb MPPs (Figure 7D) are in concordance with such a preleukemic state of the cells. It is also possible that the enhancer is involved in epigenetic deregulation of the *CEBPA* gene in certain AMLs. Patients with a chromosomal translocation t(8;21) present with low *CEBPA* expression levels.[14] The t (8;21) generates the AML1-ETO (ie, the *RUNX1-RUNX1T1* fusion transcript) fusion protein that binds to sites that are usually bound by RUNX1. The +42-kb enhancer carries multiple RUNX1-binding sites and ChIP-seq experiments in CD34^{+} cells revealed that RUNX1 binds to the enhancer (Figure 3). Knockdown of *RUNX1-RUNX1T1* in the Kasumi-1 cell line demonstrated a significant upregulation of *CEBPA* mRNA and protein levels[57] but the mechanism by which this happens has not been resolved. Our data suggest that the +42-kb enhancer is a major interaction site for

AML1-ETO, which may deregulate *CEBPA* expression. Interestingly, the transforming EVI1 protein (M.H., E.B., R.D., unpublished observation, October 2014) binds the +42-kb enhancer as well, emphasizing that further evaluation of the enhancer contribution to the pathogenesis of leukemia is warranted.

Acknowledgments

The authors thank Erik Kreiter for critically reading the manuscript.

This work was supported by the Dutch Cancer Foundation (KWF) (grant no. EMCR 2013-5829), Worldwide Cancer Research (grant no. 12-1309), and the Tata Memorial Trust Foundation. H.J.G.v.d.W. was supported by a Zenith grant (93511036) from the Netherlands Genomics Initiative.

Authorship

Contribution: R.A., E.B., and R.D. conceived of and designed the study; M.R., C.G., J.P., D.B., and R.D. provided study materials or patient samples; R.A., M.H., C.E., M.A.S., R.H., H.J.G.v.d.W., E.R., K.v.L., C.G., M.R., J.P., D.B., S.E., I.T., S.G., T.K., E.B., and R.D. provided data analysis and interpretation; R.A., M.H., C.E., P.M.H.v.S., C.G., D.B., T.K., H.d.L., and E.B. carried out experiments; and R.A., E.B., I.T., and R.D. wrote the manuscript.

Conflict-of-interest disclosure: The authors declare no competing financial interests.

Correspondence: Ruud Delwel, Department of Hematology, Erasmus University Medical Center, Dr Molewaterplein 50, 3015 GE Rotterdam, The Netherlands; e-mail: h.delwel@erasmusmc.nl.

References

1. Heinz S, Romanoski CE, Benner C, Glass CK. The selection and function of cell type-specific enhancers. *Nat Rev Mol Cell Biol.* 2015;16(3):144-154.
2. Miyamoto T, Iwasaki H, Reizis B, et al. Myeloid or lymphoid promiscuity as a critical step in hematopoietic lineage commitment. *Dev Cell.* 2002;3(1):137-147.
3. Pina C, Fugazza C, Tipping AJ, et al. Inferring rules of lineage commitment in haematopoiesis. *Nat Cell Biol.* 2012;14(3):287-294.
4. Sive JI, Göttgens B. Transcriptional network control of normal and leukaemic haematopoiesis. *Exp Cell Res.* 2014;329(2):255-264.
5. Iwasaki H, Akashi K. Myeloid lineage commitment from the hematopoietic stem cell. *Immunity.* 2007;26(6):26-40.
6. Beck D, Thoms JA, Perera D, et al. Genome-wide analysis of transcriptional regulators in human HSPCs reveals a densely interconnected network of coding and noncoding genes. *Blood.* 2013;122(14):e12-e22.
7. Chen L, Kostadima M, Martens JH, et al; BRIDGE Consortium. Transcriptional diversity during lineage commitment of human blood progenitors. *Science.* 2014;345(6204):1251033.
8. Heinz S, Benner C, Spann N, et al. Simple combinations of lineage-determining transcription factors prime cis-regulatory elements required for macrophage and B cell identities. *Mol Cell.* 2010;38(4):576-589.
9. van Galen P, Kreso A, Wienholds E, et al. Reduced lymphoid lineage priming promotes human hematopoietic stem cell expansion. *Cell Stem Cell.* 2014;14(1):94-106.
10. Hasemann MS, Lauridsen FK, Waage J, et al. C/EBPα is required for long-term self-renewal and lineage priming of hematopoietic stem cells and for the maintenance of epigenetic configurations in multipotent progenitors. *PLoS Genet.* 2014;10(1):e1004079.
11. Iwasaki H, Mizuno S, Arinobu Y, et al. The order of expression of transcription factors directs hierarchical specification of hematopoietic lineages. *Genes Dev.* 2006;20(21):3010-3021.
12. Ma O, Hong S, Guo H, Ghiaur G, Friedman AD. Granulopoiesis requires increased C/EBPα compared to monopoiesis, correlated with elevated Cebpa in immature G-CSF receptor versus M-CSF receptor expressing cells. *PLoS One.* 2014;9(4):e95784.
13. Figueroa ME, Wouters BJ, Skrabanek L, et al. Genome-wide epigenetic analysis delineates a biologically distinct immature acute leukemia with myeloid/T-lymphoid features. *Blood.* 2009;113(12):2795-2804.
14. Pabst T, Mueller BU, Harakawa N, et al. AML1-ETO downregulates the granulocytic differentiation factor C/EBPalpha in t(8;21) myeloid leukemia. *Nat Med.* 2001;7(4):444-451.
15. Perrotti D, Cesi V, Trotta R, et al. BCR-ABL suppresses C/EBPalpha expression through inhibitory action of hnRNP E2. *Nat Genet.* 2002;30(1):48-58.
16. Radomska HS, Bassères DS, Zheng R, et al. Block of C/EBP alpha function by phosphorylation in acute myeloid leukemia with FLT3 activating mutations. *J Exp Med.* 2006;203(2):371-381.
17. Pabst T, Mueller BU, Zhang P, et al. Dominant-negative mutations of CEBPA, encoding CCAAT/enhancer binding protein-alpha (C/EBPalpha), in acute myeloid leukemia. *Nat Genet.* 2001;27(3):263-270.
18. Wouters BJ, Löwenberg B, Erpelinck-Verschueren CA, van Putten WL, Valk PJ, Delwel R. Double CEBPA mutations, but not single CEBPA mutations, define a subgroup of acute myeloid leukemia with a distinctive gene expression profile that is uniquely associated with a favorable outcome. *Blood.* 2009;113(13):3088-3091.
19. Zhang DE, Zhang P, Wang ND, Hetherington CJ, Darlington GJ, Tenen DG. Absence of granulocyte colony-stimulating factor signaling and neutrophil development in CCAAT enhancer binding protein alpha-deficient mice. *Proc Natl Acad Sci USA.* 1997;94(2):569-574.
20. Akai Y, Oitate T, Koike T, Shiojiri N. Impaired hepatocyte maturation, abnormal expression of biliary transcription factors and liver fibrosis in C/EBPα(Cebpa)-knockout mice. *Histol Histopathol.* 2014;29(1):107-125.
21. Bassères DS, Levantini E, Ji H, et al. Respiratory failure due to differentiation arrest and expansion of alveolar cells following lung-specific loss of the transcription factor C/EBPalpha in mice. *Mol Cell Biol.* 2006;26(3):1109-1123.
22. Chen W, Zhu G, Hao L, Wu M, Ci H, Li YP. C/EBPα regulates osteoclast lineage commitment. *Proc Natl Acad Sci USA.* 2013;110(18):7294-7299.
23. Chandrasekaran C, Gordon JI. Cell lineage-specific and differentiation-dependent patterns of CCAAT/enhancer binding protein alpha expression in the gut epithelium of normal and transgenic mice. *Proc Natl Acad Sci USA.* 1993;90(19):8871-8875.
24. Cooper S, Guo H, Friedman AD. The +37 kb Cebpa enhancer is critical for Cebpa myeloid gene expression and contains functional sites that bind SCL, GATA2, C/EBPα, PU.1, and additional Ets factors. *PLoS One.* 2015;10(5):e0126385.
25. Risca VI, Greenleaf WJ. Unraveling the 3D genome: genomics tools for multiscale exploration. *Trends Genet.* 2015;31(7):357-372.
26. de Laat W, Duboule D. Topology of mammalian developmental enhancers and their regulatory landscapes. *Nature.* 2013;502(7472):499-506.
27. Hübner MR, Spector DL. Chromatin dynamics. *Annu Rev Biophys.* 2010;39:471-489.
28. van de Werken HJG, de Vree PJP, Splinter E, et al. 4C technology: protocols and data analysis. *Methods Enzymol.* 2012;513:89-112.
29. Bindels EM, Havermans M, Lugthart S, et al. EVI1 is critical for the pathogenesis of a subset of MLL-AF9-rearranged AMLs. *Blood.* 2012;119(24):5838-5849.
30. Kim D, Pertea G, Trapnell C, Pimentel H, Kelley R, Salzberg SL. TopHat2: accurate alignment of transcriptomes in the presence of insertions, deletions and gene fusions. *Genome Biol.* 2013;14(4):R36.
31. Trapnell C, Roberts A, Goff L, et al. Differential gene and transcript expression analysis of RNA-seq experiments with TopHat and Cufflinks. *Nat Protoc.* 2012;7(3):562-578.
32. Lieberman-Aiden E, van Berkum NL, Williams L, et al. Comprehensive mapping of long-range interactions reveals folding principles of the human genome. *Science.* 2009;326(5950):289-293.
33. Hadrys T, Punnamoottil B, Pieper M, et al. Conserved co-regulation and promoter sharing of hoxb3a and hoxb4a in zebrafish. *Dev Biol.* 2006;297(1):26-43.
34. Michalak P. Coexpression, coregulation, and cofunctionality of neighboring genes in eukaryotic genomes. *Genomics.* 2008;91(3):243-248.
35. Jin F, Li Y, Dixon JR, et al. A high-resolution map of the three-dimensional chromatin interactome in human cells. *Nature.* 2013;503(7475):290-294.
36. Rao SS, Huntley MH, Durand NC, et al. A 3D map of the human genome at kilobase resolution reveals principles of chromatin looping. *Cell.* 2014;159(7):1665-1680.
37. Ghavi-Helm Y, Klein FA, Pakozdi T, et al. Enhancer loops appear stable during development and are associated with paused polymerase. *Nature.* 2014;512(7512):96-100.
38. Dixon JR, Selvaraj S, Yue F, et al. Topological domains in mammalian genomes identified by analysis of chromatin interactions. *Nature.* 2012;485(7398):376-380.

39. Creyghton MP, Cheng AW, Welstead GG, et al. Histone H3K27ac separates active from poised enhancers and predicts developmental state. *Proc Natl Acad Sci USA.* 2010;107(50): 21931-21936.
40. Rada-Iglesias A, Bajpai R, Swigut T, Brugmann SA, Flynn RA, Wysocka J. A unique chromatin signature uncovers early developmental enhancers in humans. *Nature.* 2011;470(7333): 279-283.
41. ENCODE Project Consortium. An integrated encyclopedia of DNA elements in the human genome. *Nature.* 2012;489(7414):57-74.
42. Bailey SD, Zhang X, Desai K, et al. ZNF143 provides sequence specificity to secure chromatin interactions at gene promoters. *Nat Commun.* 2015;2:6186.
43. Spitz F, Furlong EE. Transcription factors: from enhancer binding to developmental control. *Nat Rev Genet.* 2012;13(9):613-626.
44. Visel A, Blow MJ, Li Z, et al. ChIP-seq accurately predicts tissue-specific activity of enhancers. *Nature.* 2009;457(7231):854-858.
45. Alberich-Jordà M, Wouters B, Balastik M, et al. C/EBPγ deregulation results in differentiation arrest in acute myeloid leukemia [published correction appears in *J Clin Invest.* 2013;123(1):526]. *J Clin Invest.* 2012;122(12):4490-4504.
46. Kvon EZ, Stampfel G, Yáñez-Cuna JO, Dickson BJ, Stark A. HOT regions function as patterned developmental enhancers and have a distinct cis-regulatory signature. *Genes Dev.* 2012;26(9): 908-913.
47. Frankel N, Davis GK, Vargas D, Wang S, Payre F, Stern DL. Phenotypic robustness conferred by apparently redundant transcriptional enhancers. *Nature.* 2010;466(7305):490-493.
48. Barolo S. Shadow enhancers: frequently asked questions about distributed cis-regulatory information and enhancer redundancy. *BioEssays.* 2012;34(2):135-141.
49. Koch F, Fenouil R, Gut M, et al. Transcription initiation platforms and GTF recruitment at tissue-specific enhancers and promoters. *Nat Struct Mol Biol.* 2011;18(8):956-963.
50. Zhang P, Iwasaki-Arai J, Iwasaki H, et al. Enhancement of hematopoietic stem cell repopulating capacity and self-renewal in the absence of the transcription factor C/EBP alpha. *Immunity.* 2004;21(6):853-863.
51. Ye M, Zhang H, Amabile G, et al. C/EBPa controls acquisition and maintenance of adult haematopoietic stem cell quiescence. *Nat Cell Biol.* 2013;15(4):385-394.
52. Wölfler A, Danen-van Oorschot AA, Haanstra JR, et al. Lineage-instructive function of C/EBPα in multipotent hematopoietic cells and early thymic progenitors. *Blood.* 2010;116(20): 4116-4125.
53. Porse BT, Bryder D, Theilgaard-Mönch K, et al. Loss of C/EBP alpha cell cycle control increases myeloid progenitor proliferation and transforms the neutrophil granulocyte lineage. *J Exp Med.* 2005;202(1):85-96.
54. Phillips-Cremins JE, Sauria ME, Sanyal A, et al. Architectural protein subclasses shape 3D organization of genomes during lineage commitment. *Cell.* 2013;153(6): 1281-1295.
55. Van Bortle K, Nichols MH, Li L, et al. Insulator function and topological domain border strength scale with architectural protein occupancy. *Genome Biol.* 2014;15(6):R82.
56. Sanborn AL, Rao SS, Huang SC, et al. Chromatin extrusion explains key features of loop and domain formation in wild-type and engineered genomes. *Proc Natl Acad Sci USA.* 2015;112(47): E6456-E6465.
57. Ptasinska A, Assi SA, Martinez-Soria N, et al. Identification of a dynamic core transcriptional network in t(8;21) AML that regulates differentiation block and self-renewal. *Cell Reports.* 2014;8(6):1974-1988.